PREVIEW-PREDICTOR MODEL OF DRIVER BEHAVIOR IN EMERGENCY SITUATIONS

C. V. Kroll, Cornell Aeronautical Laboratory, Inc.

This paper summarizes a research task directed toward development of a modified version of the BPR-CAL computer simulation of automobile dynamics. In particular, a nonlinear model of driver behavior has been formulated and incorporated into a "noncollision" version of the vehicle simulation. The nonlinear formulations have been aimed at producing a closed-loop control mechanism suitable for use in the investigation of driver behavior in emergency and precollision situations, specifically those situations involving maneuvers at or near the limits of vehicle and driver control. The developed model is described, and its responses are discussed.

•EXTENSIVE RESEARCH of the dynamics of the driver-vehicle-roadway system has been conducted during the last decade. The results of this work yield considerable insight into the linear or quasi-linear relationships that describe observed driver behavior under "normal" or small disturbance driving conditions. However, such relationships do not yield valid predictions of system dynamics at or near the limits of vehicle controllability because of the highly nonlinear behavior of vehicle and driver.

In the critical or emergency period immediately preceding a potential accident, the resolution of the accident situation can be greatly altered by driver control inputs. The driver control mechanism that produces these vehicle control inputs and the resultant vehicle responses quite often exceed the range of applicability of the aforementioned linear or quasi-linear analyses. A valid model of driver behavior in these critical or emergency situations involving maneuvers at or near the upper limits of vehicle controllability will permit comprehensive investigations of accident dynamics with the ultimate goal of providing guidance for reduction of the incidence and severity of automobile accidents. To this end a nonlinear multifunctional driver model has been developed and is described here.

The driver model includes data sampling, path prediction, detection thresholds, nonlinear gains, multiple-error sampling, and decision-making logic (1). The basic vehicle model used is the well-validated, nonlinear, three-dimensional formulation of simultaneous automobile ride and cornering dynamics by McHenry and DeLeys (2). Because of the absence of linear limitations on the vehicle model, the driver model is unrestricted, except by its own limitations, in its range of performance. As yet, a detailed study of the validity of the driver model has not been conducted. However, approximate values for the model parameters have been used to perform a qualitative analysis of the model behavior. The driver model is not intended to constitute a comprehensive description of nonlinear driver behavior. It does, however, incorporate several formulations that will allow further investigation of the upper limits of stability in the driver-vehicle system.

MULTIFUNCTIONAL DRIVER MODEL

The driver model includes several modes of operation: path following, speed maintenance, speed change, and skid recovery (Fig. 1). A data-sampling scheme similar

Sponsored by Committee on Simulation of Driving Task and presented at the 50th Annual Meeting.

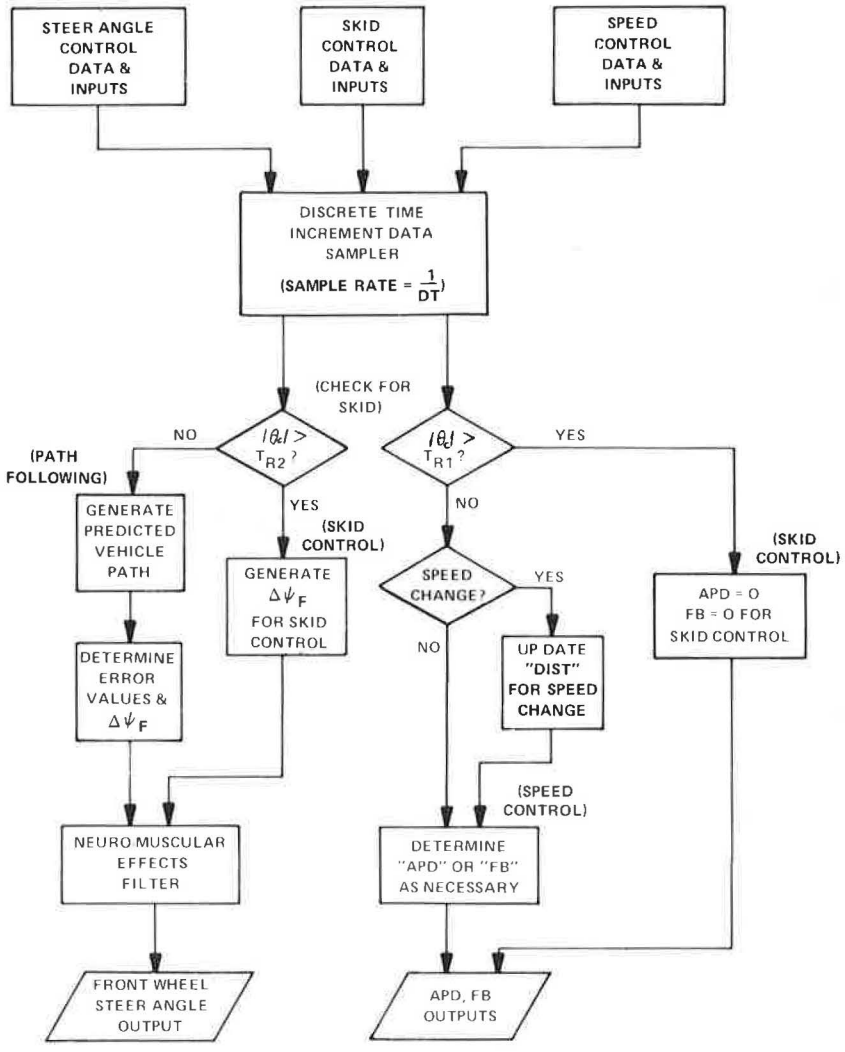

Figure 1. Model outline.

to the one investigated by Kriefeld (3) is incorporated and operates once every DT seconds. Significant changes in model output have been produced by this mechanism, including improved correlation with recorded nonlinear responses of human operators (3).

It should be noted that the threshold-indifference levels to be mentioned in the following sections are single parameters representing the minimum detection level for that particular control input or, if the driver chooses not to act until a higher value is reached, the minimum indifference level for that control input.

Path Following

The path-following mode of operation is a preview-predictor mechanism similar to those already described in the literature (4, 5, 6). The driver model predicts the vehicle position and orientation at some future time and compares this prediction with the previewed desired path to generate an error signal.

In the calculation of the predicted path, the model assumes that the vehicle will maintain its present velocity vector except for the continuous effect of the estimated

lateral acceleration, a_y, due to the front wheel steer angle, ψ_y. This estimated acceleration is calculated from the relationship

$$a_y = \frac{u_T^2 \cdot \psi_F}{L \cdot (1 + K_d \cdot u_T^2)} \tag{1}$$

where u_T is the magnitude of the vehicle velocity vector, K_d is a performance parameter characterizing the understeer-oversteer properties of the vehicle, and L is the wheelbase of the vehicle.

Error determinations, e_i, are made between the predicted and the previewed paths at N evenly spaced points, ΔS inches apart. The magnitude of the error at each point (Fig. 2) is measured in a direction perpendicular to the predicted path at that point.

The lateral acceleration required to displace the path of the vehicle by e_i at a distance d_i ahead of the vehicle is

$$a_{y_i} = 2 \cdot \frac{e_i u_T^2}{d_i^2} \tag{2}$$

Therefore, the change in front-wheel steer angle, $\Delta\psi_F$, required to nullify the error e_i is

$$\Delta\psi_F = \frac{2 \cdot L \cdot (1 + K_d u_T^2)}{d_i^2} \cdot e_i \tag{3}$$

These error estimates are weighted to account for the reduction in lateral acceleration required to nullify errors at farther distances ahead of the vehicle. If an important weighting factor is added and $\Delta S \cdot i$ is substituted for d_i, then the average required change in front-wheel steer angle, $\Delta\bar{\psi}_F$, becomes

$$\Delta\bar{\psi}_F = \frac{1}{N} \sum_{i=1}^{N} \frac{2 \cdot L \cdot (1 + K_d \cdot u_T^2)}{(\Delta S \cdot i)^2} \cdot WI_i \cdot e_i \tag{4}$$

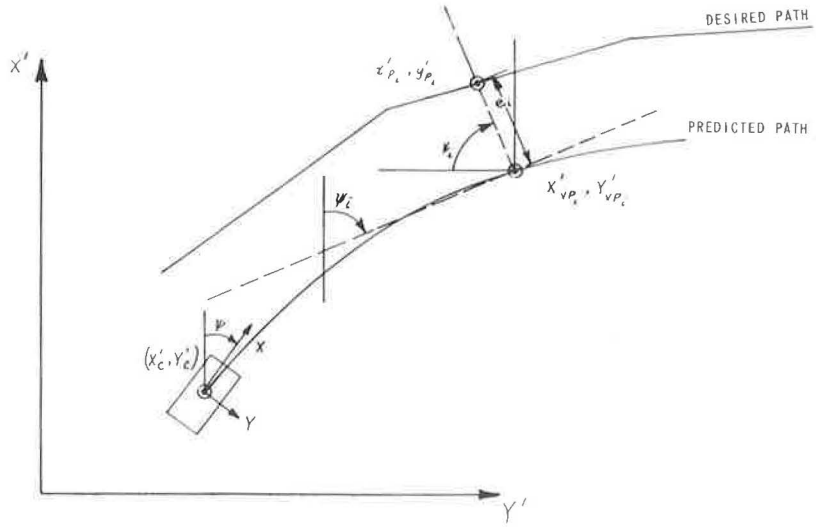

Figure 2. Error calculation.

or

$$\Delta\bar{\psi}_F = K_p \sum_{i=} WE_i \cdot WI_i \cdot e_i \tag{5}$$

where

$WE_i = 1/i^2$, error weighting function;
WI_i = importance weighting function; and
$K_p = [2 \cdot L \cdot (1+K_d u_T^2)]/(N \cdot \Delta S^2)$, control gain.

Limitations must be placed on the driver model outputs to ensure that they fall within the ranges of human dynamic capabilities. To this end a pure filter mechanism has been added to the steer output stage. This filter incorporates a time delay, τ, a possible lead term, T_L, and a lag term, T_l, each of which is a variable input of the model. This filter structure corresponds to a first-order neuromuscular model of the human operator (Fig. 3).

When this filter is incorporated, the steer output, $\Delta\psi_{F_j}(t)$, due to the error detected at time t_j, is

$$\Delta\psi_{F_j}(t) = \Delta\psi_{F_j} \left\{1 - \frac{T_l - T_L}{T_l} e^{-(1/T_l)(t - t_j - \tau)}\right\} \cdot \mu(t - t_j - \tau) \tag{6}$$

where $\mu(t - t_j - \tau)$ is the unit step function.

The time functional form of the actual steer angle is merely the sum of the j independent responses.

$$\psi_F(t) = \sum_{j=1}^{t/DT} \Delta\psi_{F_j}(t) \tag{7}$$

The front-wheel steer angle (instead of the steering wheel position) was not used previously because the available version of the vehicle model (2) did not include simulation of the steering linkage. Therefore, a simple gain mechanism was assumed and directly incorporated into the model gain.

Speed Control

Operating simultaneously with the path-following mode is either the speed change mode or the speed maintenance mode. The speed control section of the driver model is much less complex than the path-following mode.

To execute a speed change, the model determines the difference between the desired and the actual speed of the vehicles, ΔV, and attempts to nullify this difference within a prespecified distance, DIST. To accomplish this, the model determines how much time remains in which it must accomplish the task, $DIST/u_T$, and divides the velocity

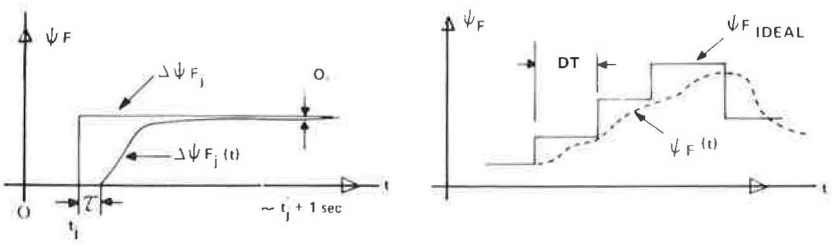

Figure 3. Neuromuscular filter characteristics.

error by this time, yielding a desired rate of acceleration, D_{ax}. That is,

$$D_{ax} = \frac{\Delta V}{(DIST/u_T)} \tag{8}$$

At each sample time DIST is updated to reflect the distance that the vehicle moved, and u_T is redetermined to reflect the effects of the acceleration. For a speed maintenance task, DIST is not periodically updated; therefore, the desired acceleration is proportional to the velocity error times the vehicle velocity.

The driver model assumes that the vehicle will experience actual accelerations that are linearly proportional to accelerator pedal deflection, APD, and the applied brake pedal force, FB, and applies the appropriate inputs to the vehicle torque systems.

Threshold-indifference levels T_{a1} and T_{a2} are applied for positive and negative ΔV levels respectively as well as a braking indifference level, T_b. When $D_{ax} < -T_b$ the model applies the brakes, in addition to decreasing the accelerator pedal deflection to zero, in an effort to reduce vehicle speed.

Skid Recovery

The skid-recovery mode of model behavior is activated only if the vehicle slip angle, θ_c, exceeds a threshold-indifference level, T_{R1} (Fig. 4). The severity of the skid is determined by comparison of θ_c with a second (higher) threshold, T_{R2}. For skids of low severity ($T_{R1} < \theta_c < T_{R2}$), the brake pedal force and accelerator pedal deflection are set to zero; the steering control remains under the path-following mode. If the skid is of high severity ($\theta_c > T_{R2}$), the driver model abandons the path-following mode and, instead, attempts to orient the vehicle so that its heading is colinear with its velocity vector. This is done by means of a simple gain mechanism operating on the error between the front-wheel steer angle and the vehicle slip angle. These steer commands are filtered, as in the path-following mode, before being applied to the vehicle.

SAMPLE RUNS

Several computer runs representing typical driving maneuvers were selected for initial check-out of the driver model. The particular maneuvers were chosen because of their relationship to the resolution of critical and emergency situations and also because of the ease with which they may be experimentally validated.

The first example was a constant velocity run at 30 mph along path A, a straight-line path with a step change of 12 ft. This maneuver demonstrates an emergency lane-change situation. The sample run shown in Figure 5 exhibits relatively minor overshoot and has a correspondingly small error-correction phase after the primary maneuver. Other runs along this path (not shown) were conducted with various combinations of the total number of sample points along the predicted path, N, and the control gain, K_p. These runs showed that the model output was smoothed with increasing N up to a maximum value of 7, beyond which negligible change occurred in the output. Variation of K_p demonstrated all regions of stability from totally unstable, through oscillatory, to critically damped response.

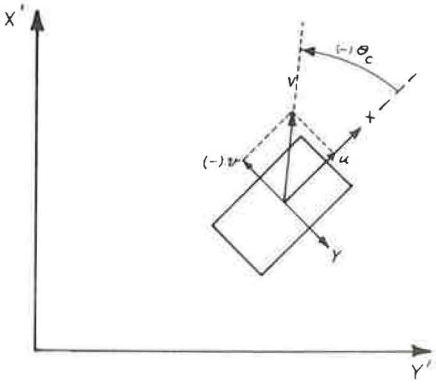

Figure 4. Vehicle slip angle.

The second example run was along a constant straight-line path and involved two speed changes from an initial speed of 8 mph. An increase to 40 mph was attempted within 166.7 ft at 0.3 sec and then a decrease to 8 mph within 83.3 ft was attempted at 5.0 sec. The initial speed change from 8 mph to 40 mph was completed in 134 ft (Fig. 6). The model then entered the speed maintenance mode at 40 mph. At 5.0 sec into

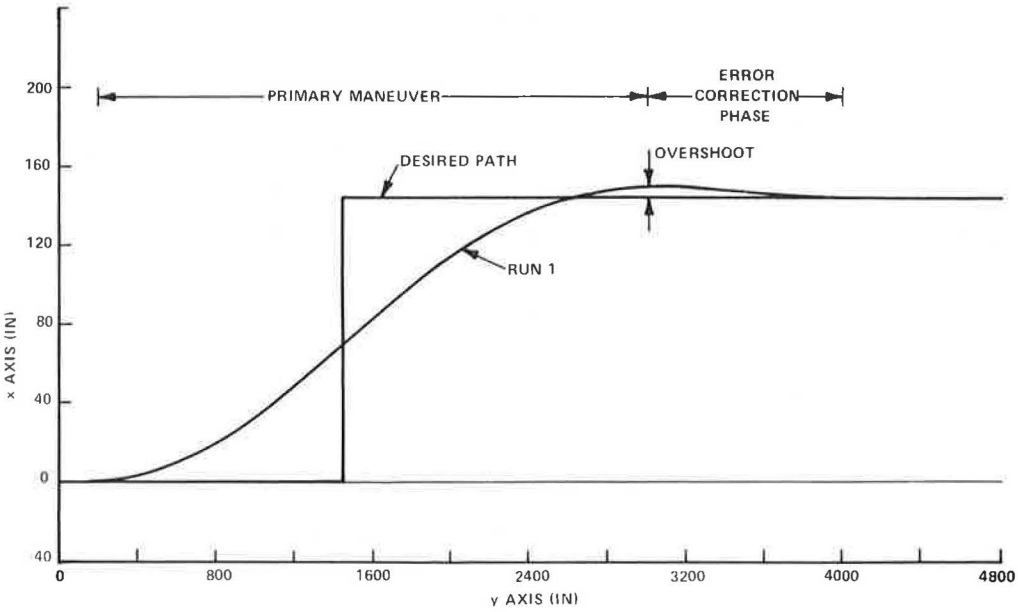

Figure 5. Vehicle path—run 1.

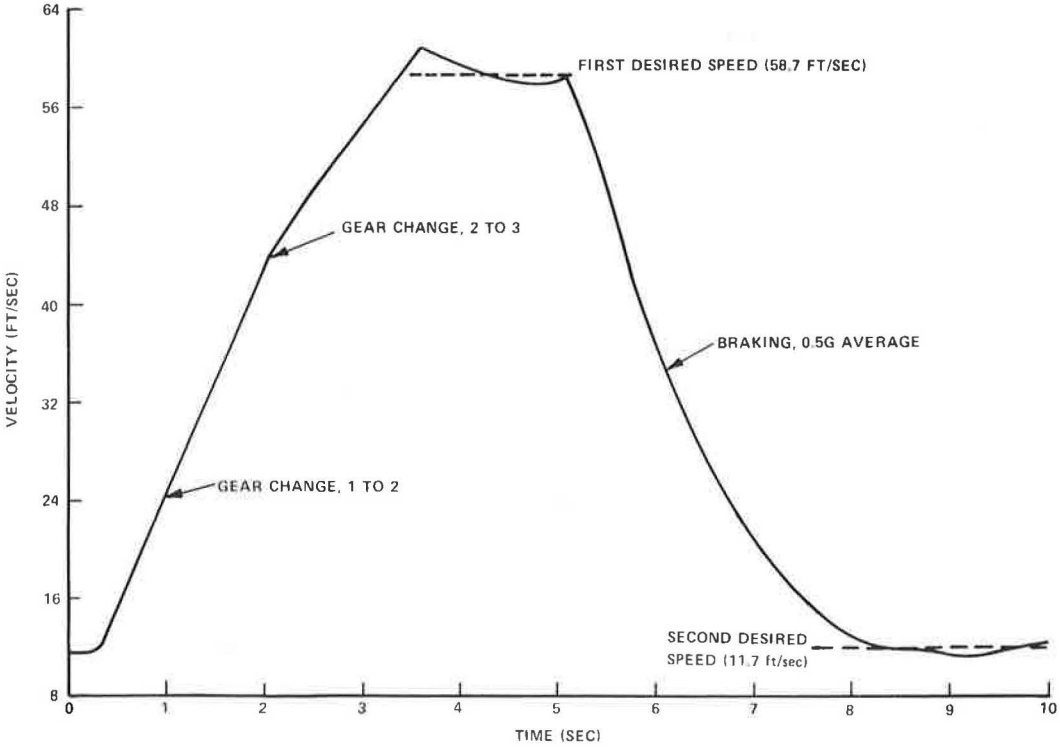

Figure 6. Vehicle speed—run 2.

the run, the deceleration was initiated and the final desired speed was reached within 95 ft. Once again the model entered the speed maintenance mode, where it remained until completion of the run.

The discrepancies between the desired distances and the actual distances are due to a method of updating DIST for the speed-change mode and also to the fact that u_T is set equal to the vehicle forward velocity at the beginning of each sample period and thus, for that period, gives an underestimate of the vehicle speed for the acceleration calculations and an overestimate for the deceleration calculations.

A series of 3 runs, examples 3, 4, and 5, involved tracking path B, a left turn with an average radius of approximately 200 ft over level terrain. For run 3 a constant speed of 30 mph was maintained. For run 4 a speed change from 30 mph to 0 mph within 60 ft, initiated 5.0 sec into the run, was also executed. Run 5 involved a skid-recovery maneuver at 40 mph. The vehicle paths for these runs are shown in Figure 7, along with the desired path.

A comparison of runs 3 and 4 illustrates the effects of vehicle speed in otherwise identical maneuvers. Figure 8 shows a comparison of front-wheel steer angles for the two runs. It can be seen that, as the vehicle in run 4 slowed to a stop, both the amplitude and frequency of the steer angle commands were reduced until a final steady value of -2.1 deg was achieved as the vehicle came to rest before completing the turn. It was originally expected that the braking action during the turn would induce a skid and allow the driver model to exercise the skid-control routine. However, although there was a significant increase in the vehicle slip angle and yaw velocity when the brakes were applied (Figs. 9 and 10), the application was not sufficient to induce skidding.

In run 5 the initial vehicle velocity was sufficiently high to induce a rear-wheel-first skid during the attempted cornering maneuver. The skid was successfully detected by

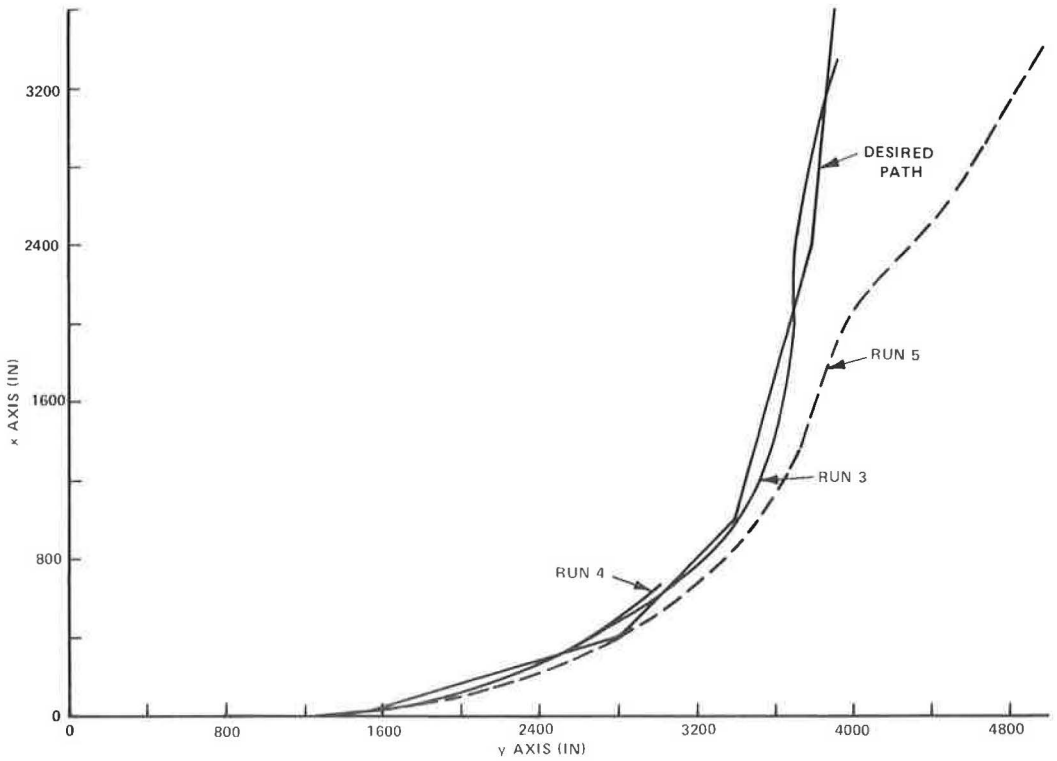

Figure 7. Vehicle paths–runs 3, 4, and 5.

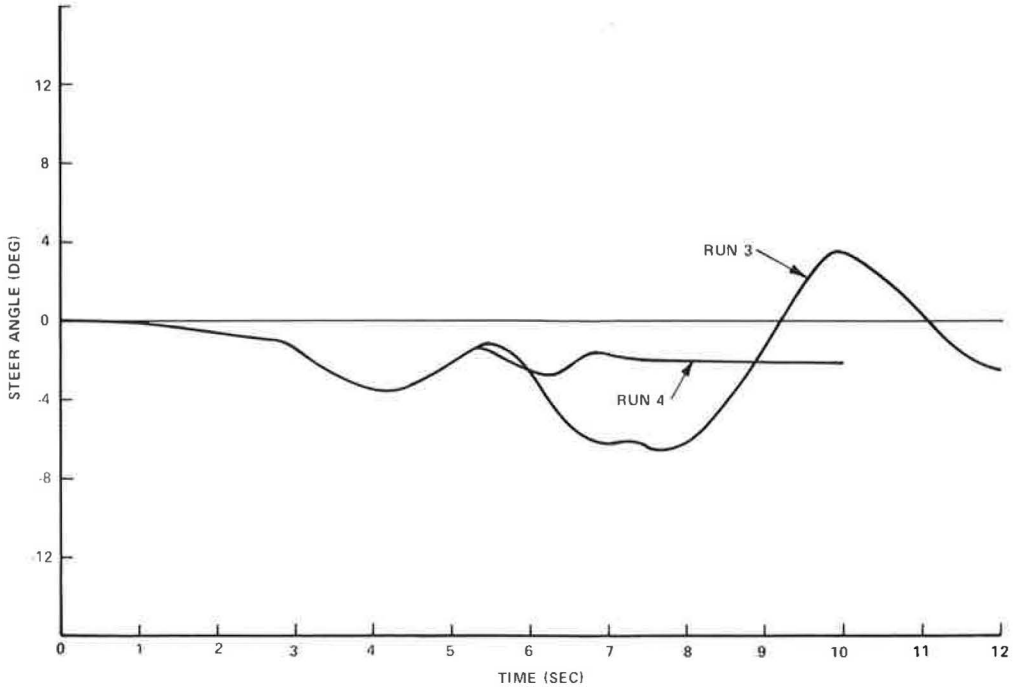

Figure 8. Front-wheel steer angles–runs 3 and 4.

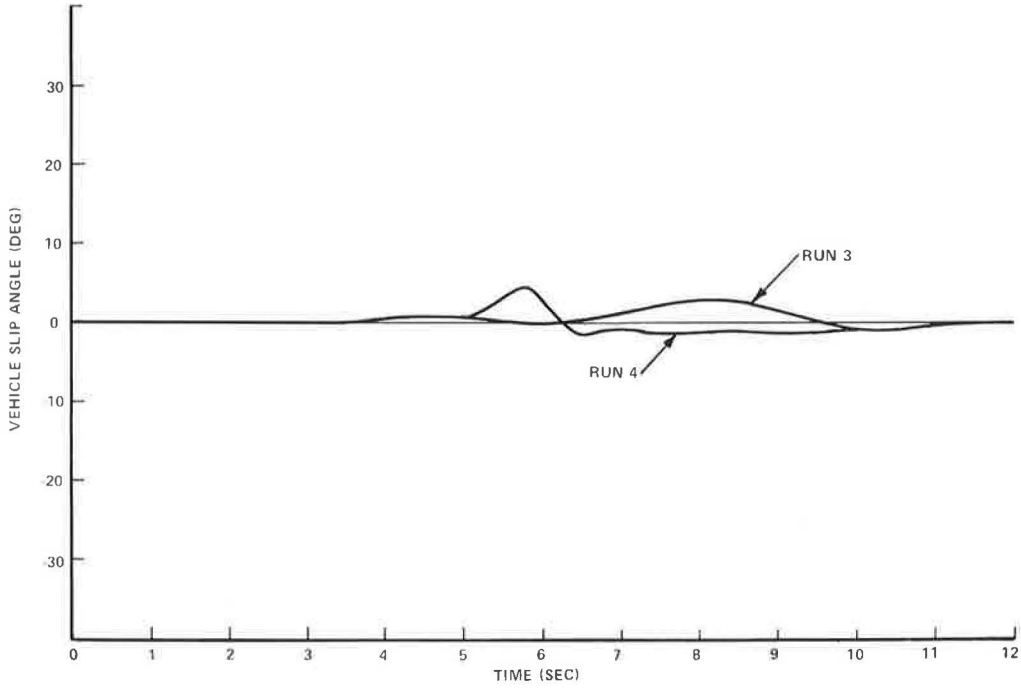

Figure 9. Vehicle slip angles–runs 3 and 4.

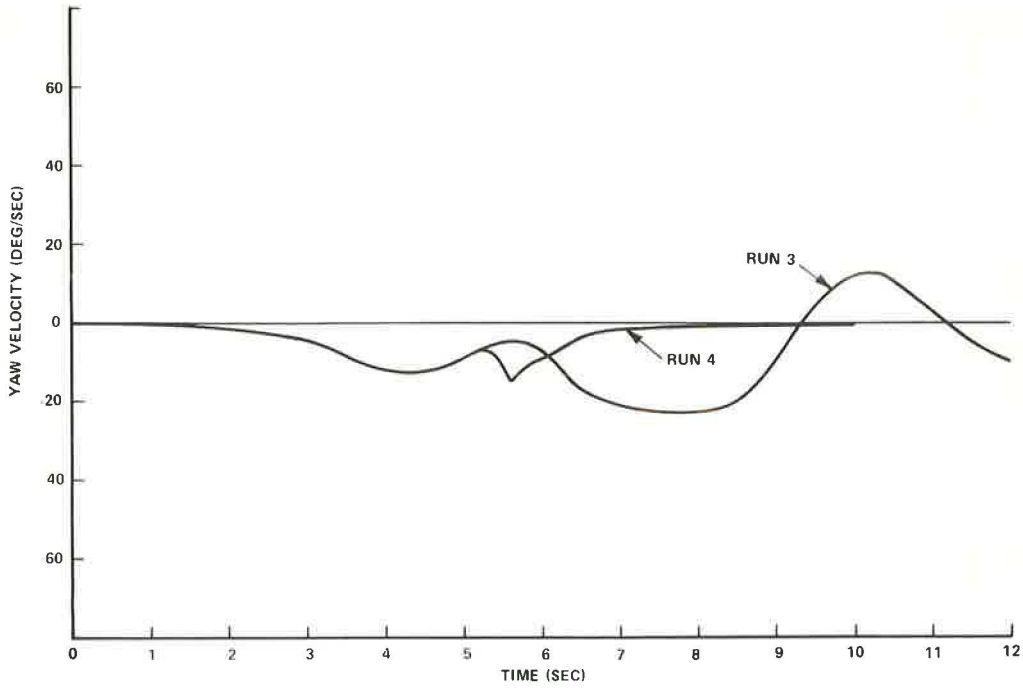

Figure 10. Yaw velocities—runs 3 and 4.

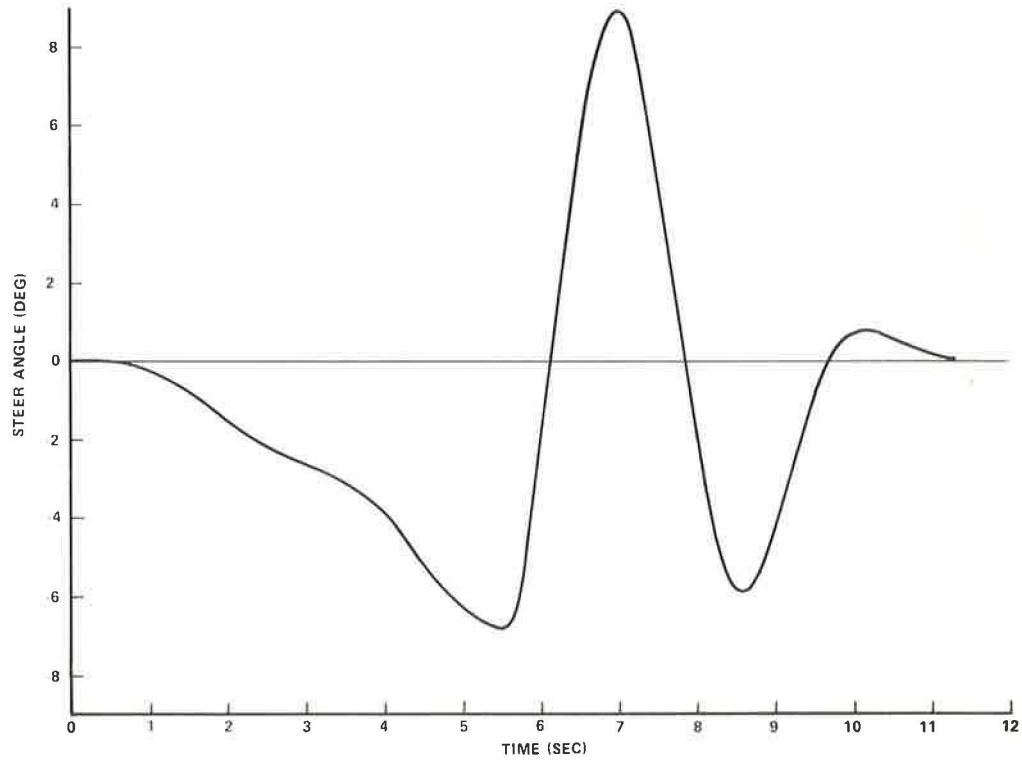

Figure 11. Front-wheel steer angle—run 5.

the driver model and the appropriate skid control maneuvers were initiated. Because both skid thresholds were exceeded, the model responded simultaneously with the proper wheel torque commands and steer angle commands. A minor programming error prevented the model from reentering the path-following mode. Instead, it continued to track the vehicle velocity vector until the end of the run.

Variations in the skid control gain, K_s, produced variations in the degree of success in controlling the skid. Figure 11 shows a time history of the front-wheel steer angles for a successfully controlled skid. From this and other runs with various values of K_s, it was shown that a gain, which is either too high or too low, will result in instability and aggravation of the skid.

CONCLUSIONS AND OBSERVATIONS

The results of the check-out runs have demonstrated several aspects of the model behavior. The model has successfully exercised all phases of driver control of the simulated vehicle, including path-following, speed-maintenance, speed-change, and skid-recovery maneuvers.

Through these and other runs it has been shown that the model responds in the manner expected of human drivers for all situations tested thus far. The model is sensitive to the extent of visibility and type of task. For example, it was found that having the error farther ahead of the vehicle more heavily weighted resulted in better performance along path A. However, weighting the error close to the vehicle more heavily weighted resulted in better performance along path B. These weightings would correspond to sighting farther down the road to correct straight-lane positioning and concentrating more heavily on the road immediately in front of the vehicle for turns and curves.

By varying the threshold levels for indifference to errors and the control gains, the apparent awareness of the driver model can be altered, including significant variations in skid-control ability. Identical circumstances were used to vary the simulated performance from virtually no loss of vehicle control to complete inability to guide the vehicle.

The smoothness with which the model operates is also variable. It was found that increasing the number of sample points tended to smooth the driver model steer output. However, an increase of the number of sample points to more than seven was found to have no effect on the motion of the vehicle.

As stated previously, no detailed correlation of driver behavior with model output has been conducted as yet primarily because of the lack of published data compatible with the nature of the proposed model.

ACKNOWLEDGMENTS

This research is being supported by the Federal Highway Administration, U.S. Department of Transportation. The opinions, findings, and conclusions expressed in this report are those of the authors and not necessarily those of the sponsor.

REFERENCES

1. Kroll, C.V., and Roland, R.D., Jr. A Preview-Predictor Model of Driver Behavior in Emergency Situations. Cornell Aeronautic Laboratory, Inc., CAL Rept. VJ-2251-V-6, Oct. 1970.
2. McHenry, R.R., and DeLeys, N. Vehicle Dynamics in Single Vehicle Accidents—Validation and Extensions of a Computer Simulation. Cornell Aeronautic Laboratory, CAL Rept. VJ-2251-V-3, Dec. 1968.
3. Kriefeld, J.G. A Sampled-Data Pursuit Tracking Model. IEEE, Trans. on Human Factors in Electronics, Sept. 1965.
4. Johnson, W. Two-Time-Scale Predictor Model Using Scan of Anticipated Inputs. Department of Mechanical Engineering, M.I.T., Cambridge, master's thesis, 1965.
5. Sheridan, T.B., Johnson, W.M., Bell, A.C., and Kreifeldt, J.C. Control Models

of Creatures Which Look Ahead. Proc., Fifth Nat. Symp. on Human Factors in Electronics, San Diego, May 1964.

6. Bekey, G., and Angel, E. S. Asynchronous Finite State Models of Manual Control Systems. National Aeronautics and Space Administration, NASA SP-128, 1966.